ISSN 1819-7124, Neurochemical Journal, 2024, Vol. 18, No. 3, pp. 483–491. © Pleiades Publishing, Ltd., 2024.

EXPERIMENTAL ARTICLES

Prenatal Ruxolitinib Treatment Improved Muscle Strength but Showed No Impact on the Neurobehavioral and Electrophysiological Traits in Adult Mice

Mansour Azimzadeh[a], Shi-En Lim[a], Nurul Syahirah Binti Mazhar[a], King-Hwa Ling[a, c, *], and Pike-See Cheah[b, c, **]

[a] *Department of Biomedical Sciences, Faculty of Medicine and Health Sciences, Universiti Putra Malaysia, UPM Serdang, Selangor, 43400 Malaysia*

[b] *Department of Human Anatomy, Faculty of Medicine and Health Sciences, Universiti Putra Malaysia, UPM Serdang, Selangor, 43400 Malaysia*

[c] *Malaysian Research Institute on Ageing (MyAgeing™), Universiti Putra Malaysia, UPM Serdang, Selangor, 43400 Malaysia*

**e-mail: lkh@upm.edu.my*

***e-mail: cheahpikesee@upm.edu.my*

Received January 27, 2024; revised April 21, 2024; accepted April 23, 2024

Abstract—The JAK/STAT signalling pathway is essential for cell communication and gene expression, particularly in brain development. Its dysregulation relates to neurological conditions such as Down syndrome and Noonan syndrome, impacting the shift from neuron to astrocyte production. Ruxolitinib, an FDA-approved JAK1 and JAK2 inhibitor, is used to treat disorders associated with dysregulated JAK-STAT signaling. This study aimed to evaluate the possible effects of prenatal ruxolitinib treatment on wild-type C57BL/6 mice, their motor skills, neurobehavioral tests, and electrophysiological properties of hippocampal CA1 neurons during adulthood. Pregnant mice were administered non-toxic doses of ruxolitinib (30 mg/kg/day) orally from E13.5 to E20.5, and nine pups were delivered for each untreated and treated group for downstream analyses. Neurobehavioral and electrophysiological experiments were performed on 8.5–10.5-week-old mice. Administering ruxolitinib prenatally significantly improved muscle strength ($p < 0.05$). However, no changes were observed in learning ability, motor coordination, locomotor function, exploratory and anxiety-related behaviour, or recognition memory ($p > 0.05$). Additionally, there were no significant differences in the input/output (IO) function or paired-pulse paradigm in hippocampal CA1 ($p > 0.05$). In conclusion, prenatal ruxolitinib treatment in C57BL/6 mice shows no adverse effects on behavioral, learning and memory but enhances muscle strength.

Keywords: electrophysiology, learning and memory, neurobehavioral, prenatal, ruxolitinib, JAK-STAT

DOI: 10.1134/S1819712424700168

INTRODUCTION

Ruxolitinib, a JAK1 and JAK2 inhibitor, gained FDA approval in November 2011 for treating intermediate- or high-risk myelofibrosis [1]. It is beneficial for polycythemia, psoriasis (topical), myelofibrosis, and cancers [2, 3]. It exhibits potent anti-inflammatory and immunosuppressive properties [4], broadening its potential application beyond hematologic conditions to various inflammatory disorders and malignancies.

The Janus kinase signal regulates cell signalling, transmitting signals from cell-membrane receptors to the nucleus [5]. It mediates cellular responses to cytokines and growth factors, influencing various cellular functions [6, 7]. The JAK/STAT signaling system consists of JAKs and STATs as ligand-receptor complexes [8]. When extracellular ligands bind to the receptor, it activates a series of conformational changes, leading to JAK autophosphorylation, recruitment of STAT proteins, dimerization, and translocation of tyrosine-phosphorylated STATs into the nucleus to regulate cellular functions [9]. Ruxolitinib inhibits JAK activity by competing with the ATP-binding catalytic site of the kinase domain. Ruxolitinib suppresses the proliferation of vascular smooth muscle cells by inhibiting JAK2/STAT3 both in vivo and in vitro [10]. In addition, it has been found to decrease cell proliferation, promote apoptosis, and suppress tumour growth in preclinical models of cisplatin-resistant non-small-cell lung cancer [11].

Studying the role of the JAK-STAT signaling pathway in brain development during pregnancy is essential for understanding its potential impact on neurodevelopment [12]. The JAK-STAT pathway regulates the production of astrocytes from neural progenitor cells

during astrogliogenesis. STAT proteins promote the expression of glial fibrillary acidic protein (GFAP), a marker of astrocyte differentiation. This is crucial for supporting the developing brain, as astrocytes play a vital role in synaptic support, clearing neurotransmitters, and establishing the blood-brain barrier. Targeting the JAK-STAT signaling pathway can potentially regulate the transition from neurogenesis to gliogenesis [13–15]. Dysfunctional activation of this pathway may contribute to neurodevelopmental disorders (e.g., Down syndrome, autism, epilepsy, fragile X mental retardation, Rett syndrome, and Alexander's disease) [16], and neurodegenerative diseases (e.g., Alzheimer's and Parkinson's diseases) [17]. Exploring its involvement in brain development could lead to discovering new therapeutic targets and interventions to mitigate its impact.

In our previous study, we administered ruxolitinib to mice from the embryonic days E7.5 to E20.5 [18], covering a broad span of embryonic to fetal development. This treatment successfully suppressed astrogliogenesis at birth and improved learning and memory in pups when they turned 2–3 months old. While the outcomes were desirable in mice, applying such therapy in human fetuses could be difficult and ethically challenging. In humans, the first trimester of pregnancy (0–90 days) corresponds to E0.5–E10.5 days in mice, while the second trimester (91–180 days) and third trimester (181–270 days) of pregnancy correspond to E11–E21 days in mice [19]. Based on multicenter trials, the first-trimester screening, conducted between 11 and 14 weeks of pregnancy, is effective and reliable for detecting Down syndrome and trisomy 18 [20]. However, amniocentesis is usually performed between the 15th and 20th weeks of pregnancy (https://www.NHS.uk/; https://www.CDC.gov/). Therefore, to address ethical concerns about the transition of the results of E7.5 treatment in mice, we are testing the possible effects of prenatal treatment at E13.5 to correspond with the 2nd trimester of pregnancy in humans.

While most research has focused on therapy for postnatal or adult patients, there is a growing interest in the potential for prenatal treatment. In this study we evaluated the potential efficacy of prenatal ruxolitinib treatment on anxiety, motor coordination, and learning and memory in C57BL/6 adult mice as a proof of concept. We conducted behavioral and electrophysiological experiments on the treated and control adult mice and found that ruxolitinib prenatal treatment had no significant impact on neurobehavioral and electrophysiological measures, except for an improvement in muscle strength.

MATERIALS AND METHODS

Animal Ethics

All procedures and experiments complied with guidelines approved by the Institutional Animal Care and Use Committee (IACUC) of Universiti Putra Malaysia (UPM) under reference number UPM/IACUC/AUP- R033/2021.

The mice were housed in individually ventilated polycarbonate cages with unidirectional sterile airflow at controlled temperature (25°C) and humidity (40–60%) in the Medical Genetics Laboratory, Faculty of Medicine, and Health Sciences at UPM. They were on a 12:12 hour light/dark cycle and had access to pellets (Altromin 1324) and autoclaved distilled water ad libitum.

Dosage and Preparation of Ruxolitinib

The concentration of ruxolitinib (MedChem Express LLC, USA) used was 60 mg/ml, dissolved in dimethyl sulfoxide (DMSO). The prenatal treatment dosage given was 30 mg/kg/day, which is non-toxic to pregnant mice [18]. Ruxolitinib was administered orally once daily via gavage with 1% (w/v) methylcellulose (Amresco) formulated in sodium chloride.

Prenatal Ruxolitinib Treatment

Female C57/BL6 mice (19–27 g, 8–10 weeks old) were mated overnight with stud males. The presence of a vaginal plug in female mice the next day confirmed successful mating, referred to as embryonic day (E) 0.5. Pregnant females were then randomly divided into two groups: the control group received 1% (w/v) methylcellulose in saline, and the treated group received 30 mg/kg of ruxolitinib in methylcellulose. All treatments were administered daily via single oral gavage (a 22G steel needle with a ball tip) between E13.5 and E20.5 of the gestational period (Fig. 1).

Behavioural Experiments

The pups were delivered between E20.5 and E21.5 and stayed with their mother for 21 days before being separated into same-sex groups after weaning. They were allowed to reach adulthood (P60–P75) without further interventions. Nine pups were in each group (control and treated) and subjected to behavioral tests. The tests were conducted between 8.00 a.m. and 7.00 p.m., and the behavioural testing apparatus was cleaned with 70% ethanol between each trial to remove any olfactory cues. The behavioral tests included rotarod, hanging wire, open field, novel object recognition and Morris water maze, performed in the order shown in Fig. 2. The procedure for each behavioural test was previously described [18]. Here, we provide a brief overview of each procedure.

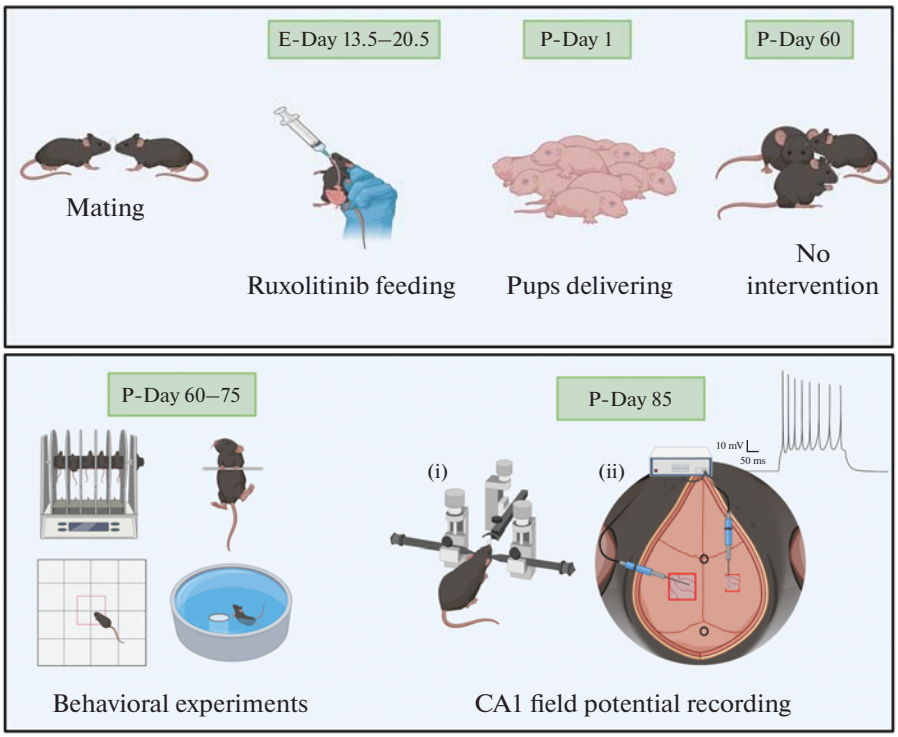

Fig. 1. Schematic representation of the experimental design showing the prenatal treatment with ruxolitinib from E13.5 to E20.5 gestational period. After birth, the pups were allowed to grow and mature without additional intervention before conducting behavioral and electrophysiological assessments. This figure was created with BioRender.com.

Rotarod and hanging wire tests. The mice's motor coordination and balance were assessed using the rotarod test, which involved three trials over three days at both fixed (4 rpm for 60 s) and accelerated (4–64 rpm over 120 s) velocities. The mice were placed on a rotating rod with five lanes, and the trial ended when they fell off, with the time recorded. A hanging device was constructed using two vertical platforms (35 cm above the ground) connected by a 30 cm long, 0.2 cm diameter metal wire. The mice were suspended by their forelimbs from the wire, and the number of falls within 180 s was recorded. This was repeated twice over two days.

Open field test. The test is commonly used to evaluate anxiety, exploration, and locomotion in mice. A 37 × 26.5 × 23 cm wall-enclosed box was used for the test, with the base divided into ten marked areas. The outer sections (areas 1–4 and 6–9) were considered safe for mice, and the open centre area (areas 5 and 10) were considered less secure. Mice naturally avoid the open areas. Each mouse was placed in the centre of the field (area 10), and the time and distance travelled in each area were recorded and analyzed using an automated video tracking system (ANY-Maze) over a 10-minute period.

Morris water maze. The spatial learning and long-term memory of the mice were assessed using the Morris water maze. The maze consisted of a 120 cm diameter black tank filled with tap water at 21–23°C. Four main positions (+ north, ★ south, ▲ east, and ■ west) were marked with visual cues, and an escape platform was placed in the middle of the northeast quadrant, hidden 1.5 cm under opaque water. The mice underwent six training days with three trials per day from different entry directions, followed by a probe trial. During training, each mouse had one minute to find and stay on the platform (for a minimum of 5 s) and an additional one minute remain on the platform to observe the visual cue. In the probe trial, the platform was removed, and the time or distance travelled to the escape platform was recorded. A visual test was also conducted to ensure the mice were not visually impaired.

Electrophysiological Studies

Surgery. Stereotaxic surgery and in vivo field potential recording were conducted with minor modifications from our recent study [21]. Mice were anaesthetized with urethane (1.2 g/kg, intraperitoneal, Sigma-Aldrich Co., USA) and then placed on a stereotaxic device. A craniotomy was performed using stereotaxic coordinates [22] to place stimulating and recording electrodes. We used stainless-steel Teflon isolated wire (Model 91.500, A-M Systems Inc., USA) for both electrodes. A bipolar stimulating electrode

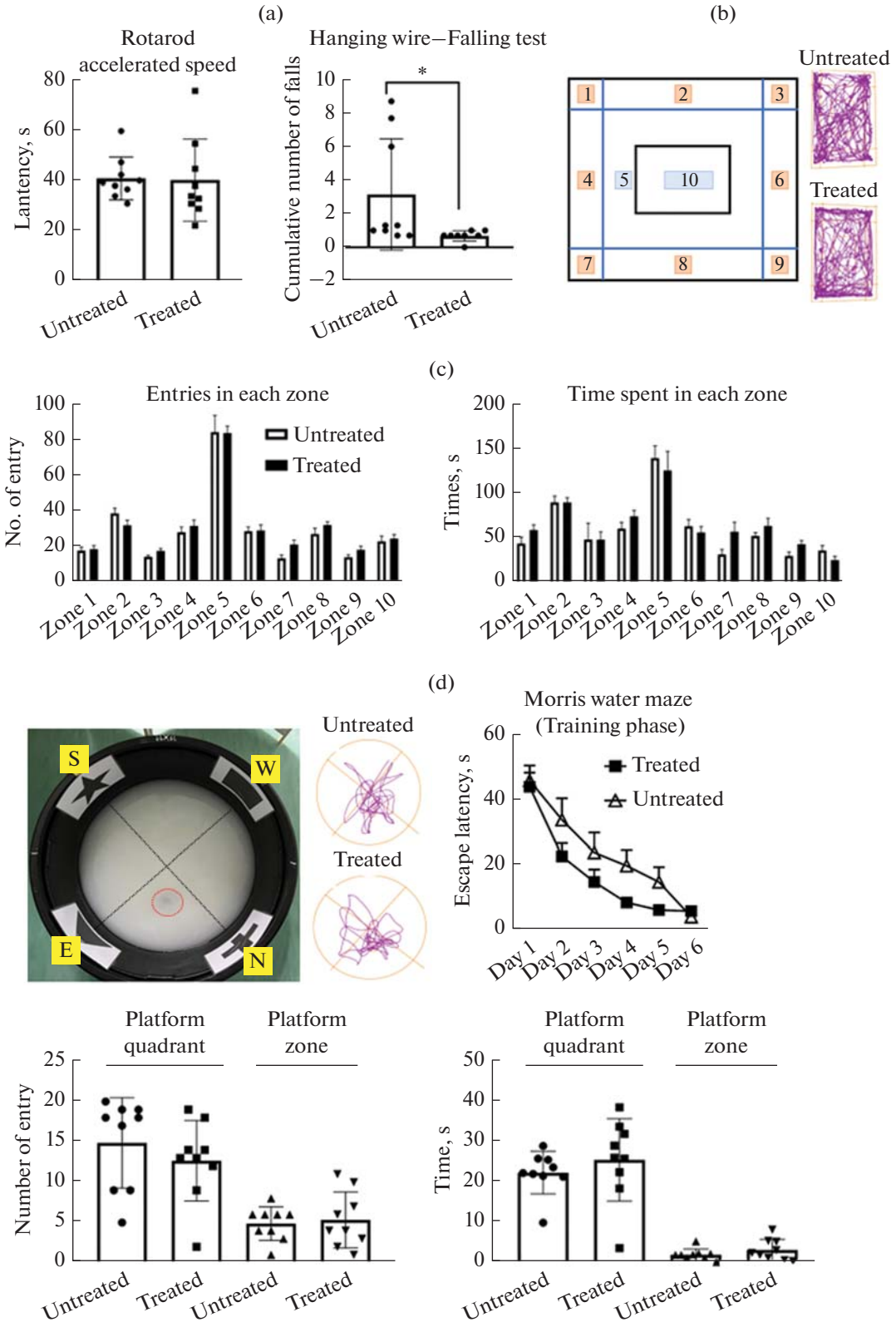

Fig. 2. (a) Rotarod and hanging wire tests. The measurements of locomotor coordination (rotarod) and forelimb strength (hanging wire test). (b) Open field test. The open-field test measures exploratory behaviour and overall levels of hyperactivity and anxiety in mice. Representative animal locomotion tracking for both the untreated and treated groups. (c) The data shows the number of entries and the time spent in each zone in the open-field test (unpaired *t*-test). (d) Morris water maze test. Representative animal locomotion tracking for both the untreated and treated groups. Travelled distance during 6 days of training phase. Time spent in the platform quadrant, number of entries to the platform quadrant, time spent in the platform zone and number of the entry to the platform zone during the probe test on day 7. All values represent mean ± SD; * denotes $p < 0.05$. Each experiment included 9 animals in each group.

was placed on the right Schaffer collateral pathway (AP: −1.5, ML: +2, DV: 1−1.5 mm from dura), and a unipolar recording electrode was placed on the right CA1 (AP: −2.2, ML: +1.2, DV: 1.8−2.5 mm from dura). The unipolar recording electrode was lowered from the left side of the skull into the right CA1 region at a 55°C angle. The bregma was the origin point for the anterior-posterior (AP) and mediolateral (ML) coordinates.

In vivo field excitatory postsynaptic potential (fEPSP). Field EPSPs were evoked by electrical pulses delivered at 0.1 Hz stimulation. The signals were amplified at ×1000 with a bandwidth of 1 Hz−3 kHz using a constant current stimulator device, e-Pulse (Science Beam, Tehran, Iran). The signals were recorded by e-Wave (Science Beam, Tehran, Iran) and processed offline using eTrace Analysis software (Science Beam, Tehran, Iran). Test pulses were applied with a 100-ms, square, monophasic single pulse to determine the maximum fEPSP at the Schaffer collateral-CA1 synapse.

Input/output (IO) function. To evaluate the IO function, mice were stimulated with 100 μs duration, square, single pulses of increasing intensity (50−400 μA, in steps of 50 μA) at the Schaffer collaterals-CA1 synapses to create IO curves. Five pulses of each intensity were presented to the animals at intervals of 30 s, and the average response was used to develop the IO curve. The stimulation intensity used to assess the paired-pulse facilitation and LTP function was considered to be 30−40% of the intensity required to evoke the maximum fEPSP response.

Paired pulse paradigm. To evaluate paired-pulse facilitation, pairs of pulses with interstimulus intervals of 10, 20, 40, 100, 200, and 500 ms (five pulses each) were used to stimulate mice.

Histology. The mice were perfused transcranially with saline and 10% buffered formalin. The brain was fixed in 10% buffered formalin for 2−3 days and then sliced into 50 μm thick coronal sections. These sections were used for histologically verifying the electrode placement at the end of the electrophysiological investigation using light microscopy (Fig. 3a).

Statistical Analysis

All the data were analyzed using SPSS version 21. Parametric tests were used to check for outliers, significant differences in variances, and normality. An unpaired two-tailed t-test and a two-way ANOVA was used for comparisons involving two or more groups. Non-parametric tests (Mann−Whitney test) were used if significant differences in variances and normality tests were observed. All graphs were created using GraphPad Prism version 9. Results were considered statistically significant if the corrected p-value was < 0.05.

RESULTS

Behavioural Experiments

The behavioural experiments showed no significant differences in the latency to fall from the rotarod device within 120 s between the control and treated groups (t-value = 0.1090, df = 12.03, $p > 0.05$) (Fig. 2a). To test muscle strength, we used the hanging wire test. The data was analyzed using a two-tailed Mann−Whitney test, which showed significant differences between the treated and control groups ($p < 0.05$). This suggests that the treated mice had stronger muscle strength than the control mice (Fig. 2a).

General exploratory and anxiety-like behaviour in the animals was evaluated using open-field tests. The results showed that the control and treated groups spent similar amounts of time in each zone (outer zones 1−4 and 6−9, and centre zones 5 and 10), with no significant differences observed. In addition, the number of entries in each zone did not differ significantly between the groups (unpaired t-test, $p > 0.05$). These findings suggest that mice from both groups exhibited similar levels of anxiety-related and general exploratory behaviour (Figs. 2b−2c).

The Morris water maze was used to evaluate the spatial learning and long-term memory of mice. The two-way repeated-measures ANOVA analysis showed that both groups improved in finding a hidden platform over the six days of training, as indicated by a decrease in escape latency [F (5, 60) = 32.414, P = 0.000). Additionally, both groups exhibited a similar decrease in escape latency over the 6-day training session [F (5, 60) = 0.538, $P > 0.746$]. The analysis of the between-subject effect showed no significant differences between the untreated and treated groups [F (1, 12) = 1.308, $P = 0.275$].

After a 24-hour resting period, a probe trial was conducted where the escape platform was removed, and the mice were allowed to explore the water pool for 1 minute. There were no significant differences between the control and treated groups in terms of total distance travelled, number of entries, or time spent in the platform quadrant (unpaired t-test, $p > 0.05$) (Fig. 2d).

Electrophysiological Experiments

We examined the basic properties of the Schafer collateral − CA1 synapse by stimulating it with single pulses of increasing intensity (50−400 μA, in 50 μA steps) in IO function (Figs. 3a−3b). We evaluated both the amplitude and slope of the fEPSPs. The IO curves showed a sigmoid shape in both the control and treated groups, indicating that the fEPSP increased in direct proportion to the rise in current intensity. Statistical analysis using two-way repeated measures ANOVA revealed significant effects of the "current" for both amplitude [F (7, 105) = 61.354, $P = 0.000$] and slope [F (7, 105) = 65.846, $P = 0.000$]. However,

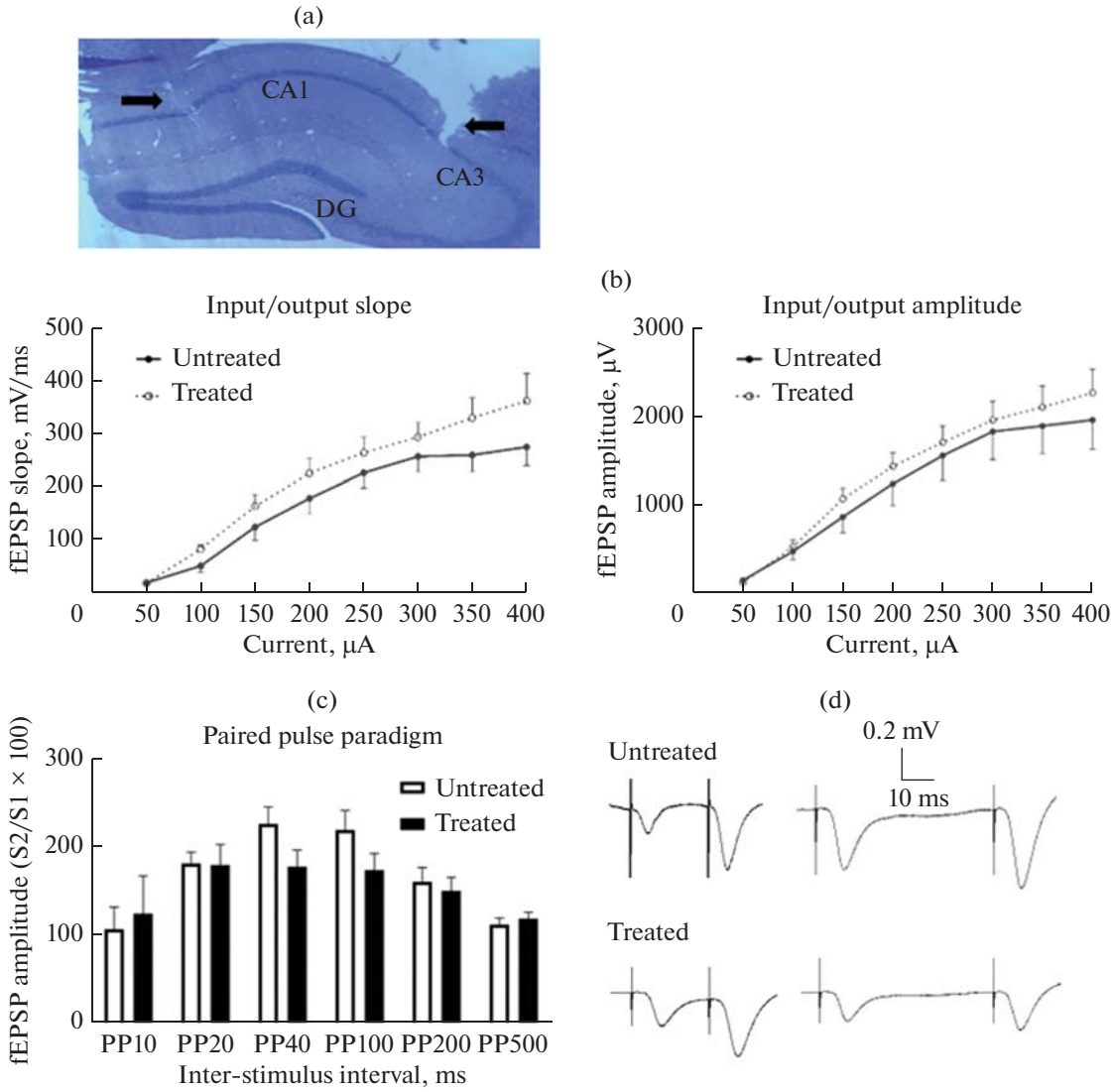

Fig. 3. Extracellular local field potential recording at the Schaffer collaterals—CA1 synapse (Untreated, $n = 9$; treated, $n = 8$). (a) Histological image of the right hippocampus. Representative micrographs illustrating the final placement of stimulating and recording electrodes, marked with a black arrow. (b) Input/output (IO) curves. Five pulses of each intensity were presented to the animals at intervals of 30 seconds to avoid stimulus interactions. No significant differences in amplitude and slope of the EPSPs were detected between groups (two way ANOVA, repeated measure, $p > 0.05$). (c) Paired-pulse paradigm. Every column represents the mean value of five stimuli (with its corresponding SEM). When the groups were compared, they presented similar patterns in the same interstimulus intervals ($p > 0.05$, unpaired t-test). (d) An example of fEPSP evoked by paired-pulse stimulation at 40 and 100 ms intervals.

there were no significant effects in the "current * group" for both amplitude [F (7, 105) = 0.307, P = 0.949] and slope [F (7, 105) = 0.942, P = 0.477], indicating a similar trend in the amplitude and slope of the IO curves between control and treated groups. There were also no significant differences in the "current effect between groups" in the amplitude [F (1, 15) = 11.349, P = 0.563] and slope [F (1, 15) = 2.053, P = 0.172] between the control and treated groups (Two-way repeated measure ANOVA) (Fig. 3b).

We also conducted a paired-pulse paradigm test with increasing interstimulus intervals (10, 20, 40, 100, 200, and 500 ms). The results showed no significant differences between the control and treated groups at different interstimulus intervals ($P > 0.05$, unpaired two-tailed t-test) (Figs. 3c–3d).

DISCUSSION

Our study found that administering ruxolitinib, JAKs inhibitor, to pregnant mice from E13.5 to 20.5 of pregnancy improved their offspring's muscle strength at the adult stage. However, it did not affect motor coordination, locomotor function, exploratory, anxi-

ety-related behavior, and learning and memory function. In addition, there were no significant differences in evaluation of IO function and paired pulse paradigm between groups.

The JAK-STAT pathway is crucial for brain development, as it mediates signals that impact neurogenesis and gliogenesis. It is also activated in central nervous system injury, playing a role in forming a glial scar in the injured area. When activated by gliogenic factors or cytokines, this pathway specifies glial differentiation and regulates astrogliogenesis, which has implications for brain development in conditions like Down Syndrome and Noonan syndrome. Dysregulation in this pathway may contribute to the altered balance between neurogenesis and gliogenesis observed in the Down Syndrome brain, thereby presenting a target for therapeutic intervention [12, 23].

Studies have reported that inhibition of this pathway blocks astrogliogenesis [24, 25]. Our previous study showed that administration of ruxolitinib during E7.5-20.5 successfully suppressed astrogliogenesis and improved learning, memory, and cognitive functions among adult mice treated prenatally [18]. Between E7.5 and E10 of the mouse gestational period, the neural tube is formed that eventually develops into the forebrain, midbrain, and hindbrain. By E11, hippocampal formation is developed. The cerebellum develops between E12 and E13 [26]. Rhombencephalon differentiates into the metencephalon and myelencephalon between E9.5 and E11.5. The metencephalon forms the cerebellum between E12 and E13.5, while the myelencephalon forms the medulla oblongata between E11.5 and E12.5 [27]. The changes from late gestation (around E15) through the first 7 to 10 days after birth in rodents are similar to those in human fetuses during the third trimester of pregnancy [28, 29]. Key changes at this stage involve the production, migration, and differentiation of additional cells in neurons and glia in certain regions [26]. Synaptogenesis begins in the third trimester and continues for a much more extended period, such as for years in human infants [30, 31]. Research indicates that there are specific areas where astrocytes are initially formed, but the exact locations and timing of their production are poorly understood. The marker for astrocytes, GFAP, is first observed in low levels in the ventricular zone at E12, and by E15, its expression increases in the periventricular regions and the hippocampus. However, at these early stages, GFAP expression is limited to radial glia and not fully developed astrocytes. By E18, the formation of astrocytes progresses, with increasing GFAP expression and the characteristic stellate morphology observed in cells throughout the brain tissue [32, 33].

During the peak stage of embryonic neurogenesis at E13.5, neural stem cells and neural progenitor cells primarily undergo asymmetric divisions to self-renew and produce either a neuron or an intermediate progenitor cell [34]. In this study, we administered ruxolitinib from E13.5 to E20.5 and found that it resulted in muscle strength. Individuals with Down syndrome and mice models often experience skeletal muscle hypotonia [35, 36]. The JAK-STAT signaling pathway plays a role in muscle development and weakness. JAK-mediated pathways are important during development and involved in muscle atrophy and regeneration. In skeletal muscle, the JAK/STAT pathway is activated by IL-6 cytokines, leading to muscle hypertrophy through increased satellite cell proliferation and muscle wasting [37, 38]. Merosin-deficient congenital muscular dystrophy in mice is characterized by poor fetal muscle development, which is linked to JAK-STAT activation, serving as a key indicator of disease initiation and progression [39]. Taken together, one encouraging finding from our studies on prenatal ruxolitinib treatment is the improvement of muscle strength observed in the treated mice. These results point to a potential application of prenatal interventions to address muscular issues associated with developmental disorders. Since musculoskeletal development begins *in utero*, the timing of treatment is critical for achieving optimal results. Our results suggest that the prenatal periods could be crucial windows for successfully mitigating muscle-related deficits that manifest in conditions like Down syndrome and muscular dystrophies.

Ruxolitinib did not impact neurobehaviour experiments, learning, or memory when administered from E13.5–20.5. However, it improved these functions when given from E7.5–20.5 [18]. Therefore, the effects of prenatal ruxolitinib treatment on neurobehavioral measures present a more complex picture. Our results indicate a lack of significant effects on anxiety, motor coordination, learning, and memory in adult offspring mice. This finding is crucial because it points out the limitations of prenatal ruxolitinib treatment in addressing specific aspects of neurological development. In vivo electrophysiology results showed that ruxolitinib given during E13.5–20.5 did not affect the IO function of the Schaffer collateral—CA1 synapse in adult offspring. This indicates that prenatal administration of ruxolitinib had no effects on the excitability of the synapse [40]. Evaluation of the paired-pulse paradigm also showed no significant differences at different inter-stimulus intervals, indicating that prenatal ruxolitinib had no effects on the short-term memory of the adult pups [41]. These results suggest that the JAK/STAT signaling pathway may not be the only factor affecting hippocampal function, despite its critical function in brain development. This raises questions about the alternative treatment periods and roles of different signaling pathways in neuronal development and how they can be influenced through prenatal drug intervention. Thus, further exploration into the timing and mechanisms of prenatal ruxolitinib treatment as well as using other JAK inhibitors (such as tofacitinib, upadacitinib, and

decernotinib) or STAT inhibitors for targeting JAK-STAT signaling pathway is warranted.

CONCLUSIONS

In this study, prenatal treatment with ruxolitinib from E13.5 to 20.5 improved muscle strength in adult offspring mice. However, it did not affect anxiety, motor coordination, learning, memory, IO function, or paired-pulse paradigm in neurobehavioural and electrophysiological experiments. Future research should focus on fully understanding the therapeutic benefits of using ruxolitinib during pregnancy, its effects on the JAK/STAT signalling pathway, and refining its usage guidelines due to the substantial potential impact of prenatal interventions.

AUTHOR CONTRIBUTION

Mansour Azimzadeh: Data curation, Formal analysis, Investigation, Visualization, Methodology, Writing—original draft. Shi-En Lim: Data curation, Formal analysis, Investigation, Visualization, Methodology. Nurul Syahirah Binti Mazhar: Data curation, Formal analysis, Investigation, Visualization, Methodology. King-Hwa Ling: Visualization, Methodology, Validation, Conceptualization, Funding acquisition, Supervision, Writing—review & editing, Project administration, Resources. Pike—See Cheah: Visualization, Methodology, Validation, Conceptualization, Funding acquisition, Supervision, Writing – review & editing, Project administration, Resources.

FUNDING

This work was supported by Universiti Putra Malaysia Geran Putra Berimpak (GP-GPB/2022/9710500) awarded to PSC.

DATA AVAILABILITY

Data will be made available on request.

ETHICS APPROVAL AND CONSENT TO PARTICIPATE

All procedures and experiments complied with guidelines approved by the Institutional Animal Care and Use Committee (IACUC) of Universiti Putra Malaysia (UPM) under reference number UPM/IACUC/AUP- R033/2021.

CONFLICT OF INTEREST

The authors of this work declare that they have no conflicts of interest.

REFERENCES

1. Quintás-Cardama, A., Kantarjian, H., Cortes, J., and Verstovsek, S., *Nat. Rev. Drug Discov.*, 2011, vol. 10, no. 2, pp. 127–140.
2. Seif, F., Khoshmirsafa, M., Aazami, H., Mohsenzadegan, M., Sedighi, G., and Bahar, M., *Cell. Commun. Signal.*, 2017, vol. 15, pp. 1–13.
3. Verstovsek, S., Mesa, R.A., Gotlib, J., Gupta, V., DiPersio, J.F., Catalano, J.V., Deininger, M.W., Miller, C.B., Silver, R.T., and Talpaz, M., *J. Hematol. Oncol.*, 2017, vol. 10, pp. 1–14.
4. Elli, E.M., Baratè, C., Mendicino, F., Palandri, F., and Palumbo, G.A., *Front. Oncol.*, 2019, vol. 9, p. 1186.
5. Renauld, J.-C., *Nature Reviews Immunology*, 2003, vol. 3, no. 8, pp. 667–676.
6. Nicolas, C.S., Amici, M., Bortolotto, Z.A., Doherty, A., Csaba, Z., Fafouri, A., Dournaud, P., Gressens, P., Collingridge, G.L., and Peineau, S., *Jakstat*, 2013, vol. 2, no. 1, p. e22925.
7. Liongue, C., O'Sullivan, L.A., Trengove, M.C., and Ward, A.C., *PLoS One*, 2012, vol. 7, no. 3, p. e32777.
8. Hu, X., Li, J., Fu, M., Zhao, X., and Wang, W., *Signal. Transduct. Target Ther.*, 2021, vol. 6, no. 1, p. 402.
9. Mascarenhas, J. and Hoffman, R., *Clin. Cancer Res.*, 2012, vol. 18, no. 11, pp. 3008–3014.
10. Song, H.T., Cui, Y., Zhang, L.L., Cao, G., Li, L., Li, G., and Jia, X.J., *Microvasc. Res.*, 2020, vol. 132, p. 104060.
11. Hu, Y., Hong, Y., Xu, Y., Liu, P., Guo, D.H., and Chen, Y., *Apoptosis*, 2014, vol. 19, no. 11, pp. 1627–1636.
12. Lee, H.C., Tan, K.L., Cheah, P.S., and Ling, K.H., *Neural Plast.*, 2016, vol. 2016, p. 7434191.
13. Sloan, S.A. and Barres, B.A., *Curr. Opin. Neurobiol.*, 2014, vol. 27, pp. 75–81.
14. Rusek, M., Smith, J., El-Khatib, K., Aikins, K., Czuczwar, S.J., and Pluta, R., *Int. J. Mol. Sci.*, 2023, vol. 24, no. 1, p. 864.
15. Huang, T., Fakurazi, S., Cheah, P.S., and Ling, K.H., *Int. J. Mol. Sci.*, 2023, vol. 24, no. 12, p. 9980.
16. Molofsky, A.V., Krencik, R., Ullian, E.M., Tsai, H.H., Deneen, B., Richardson, W.D., Barres, B.A., and Rowitch, D.H., *Genes Dev.*, 2012, vol. 26, no. 9, pp. 891–907.
17. Chandrasekaran, A., Avci, H.X., Leist, M., Kobolák, J., and Dinnyés, A., *Front. Cell. Neurosci.*, 2016, vol. 10, p. 215.
18. Lee, H.C., Hamzah, H., Leong, M.P., Md Yusof, H., Habib, O., Zainal Abidin, S., Seth, E.A., Lim, S.M., Vidyadaran, S., Mohd Moklas, M.A., Abdullah, M.A., Nordin, N., Hassan, Z., Cheah, P.S., and Ling, K.H., *Sci. Rep.*, 2021, vol. 11, no. 1, p. 3847.
19. Sones, J.L. and Davisson, R.L., *Physiol. Genomics*, 2016, vol. 48, no. 8, pp. 565–572.
20. Driscoll, D.A. and Gross, S.J., *Genet. Med.*, 2009, vol. 11, no. 11, pp. 818–821.
21. Azimzadeh, M., Mohd Azmi, M.A.N., Reisi, P., Cheah, P.-S., and Ling, K.-H., *MethodsX*, 2024, vol. 12, p. 102544.
22. Paxinos, G. and Franklin, K.B., *Paxinos and Franklin's the Mouse Brain in Stereotaxic Coordinates.*, 2019, Academic press.
23. Wang, T., Yuan, W., Liu, Y., Zhang, Y., Wang, Z., Zhou, X., Ning, G., Zhang, L., Yao, L., Feng, S., and Kong, X., *Biomed. Rep.*, 2015, vol. 3, no. 2, pp. 141–146.

24. He, F., Ge, W., Martinowich, K., Becker-Catania, S., Coskun, V., Zhu, W., Wu, H., Castro, D., Guillemot, F., Fan, G., de Vellis, J., and Sun, Y.E., *Nat. Neurosci.*, 2005, vol. 8, no. 5, pp. 616–625.
25. Cao, F., Hata, R., Zhu, P., Nakashiro, K., and Sakanaka, M., *Biochem. Biophys. Res. Commun.*, 2010, vol. 394, no. 3, pp. 843–847.
26. Chen, V.S., Morrison, J.P., Southwell, M.F., Foley, J.F., Bolon, B., and Elmore, S.A., *Toxicol. Pathol.*, 2017, vol. 45, no. 6, pp. 705–744.
27. Kaufman, M.H. and Bard, J.B., *The Anatomical Basis of Mouse Development,* 1999, Gulf Professional Publishing.
28. Workman, A.D., Charvet, C.J., Clancy, B., Darlington, R.B., and Finlay, B.L., *J. Neurosci.*, 2013, vol. 33, no. 17, pp. 7368–7383.
29. Bolon, B., *Pathology of the Developing Mouse: A Systematic Approach,* 2015, CRC Press.
30. Rice, D. and Barone, S., Jr., *Environ. Health Perspect.*, 2000, vol. 108, Suppl. 3(Suppl 3), pp. 511–533.
31. Olney, J.W., *Neurotoxicology*, 2002, vol. 23, no. 6, pp. 659–668.
32. Mamber, C., Kamphuis, W., Haring, N.L., Peprah, N., Middeldorp, J., and Hol, E.M., *PLoS One*, 2012, vol. 7, no. 12, p. e52659.
33. Liu, Y., Wu, Y., Lee, J.C., Xue, H., Pevny, L.H., Kaprielian, Z., and Rao, M.S., *Glia*, 2002, vol. 40, no. 1, pp. 25–43.
34. Noctor, S.C., Martínez-Cerdeño, V., and Kriegstein, A.R., *J. Comp. Neurol.*, 2008, vol. 508, no. 1, pp. 28–44.
35. Leong, M.P.Y., Bala, U., Lim, C.L., Rosli, R., Cheah, P.-S., and Ling, K.H., *NeurosciRN*, 2018, vol. 1, no. 1, pp. 21–41.
36. Dey, A., Bhowmik, K., Chatterjee, A., Chakrabarty, P.B., Sinha, S., and Mukhopadhyay, K., *Front. Genet.*, 2013, vol. 4, p. 57.
37. Moresi, V., Adamo, S., and Berghella, L., *Front. Physiol.*, 2019, vol. 10, p. 500.
38. Price, F.D., von Maltzahn, J., Bentzinger, C.F., Dumont, N.A., Yin, H., Chang, N.C., Wilson, D.H., Frenette, J., and Rudnicki, M.A., *Nat. Med.*, 2014, vol. 20, no. 10, pp. 1174–1181.
39. Nunes, A.M., Wuebbles, R.D., Sarathy, A., Fontelonga, T.M., Deries, M., Burkin, D.J., and Thorsteinsdóttir, S., *Hum. Mol. Genet.*, 2017, vol. 26, no. 11, pp. 2018–2033.
40. Alavi, S.M.M., Goetz, S.M., and Saif, M., *J. Neural. Eng.*, 2021, vol. 18, no. 4, p. 046071.
41. Jackman, S.L. and Regehr, W.G., *Neuron*, 2017, vol. 94, no. 3, pp. 447–464.